HHS Public Access

Author manuscript

Curr Eye Res. Author manuscript; available in PMC 2023 December 11.

Published in final edited form as:

Curr Eye Res. 2018 December ; 43(12): 1489–1499. doi:10.1080/02713683.2018.1508726.

A Small Molecule TrkB Neurotrophin Receptor Partial Agonist as Possible Treatment for Experimental Nonarteritic Anterior Ischemic Optic Neuropathy

Mohammad Ali Shariati[1], **Varun Kumar**[1], **Tao Yang**[2], **C Chakraborty**[2], **Ben A. Barres**[2,*], **Frank M. Longo**[2], **Yaping Joyce Liao**[1,2]

[1]Department of Ophthalmology, Stanford University School of Medicine, Stanford, CA, USA

[2]Department of Neurobiology, Stanford University School of Medicine, Stanford, CA, USA

Abstract

PURPOSE: Brain-derived neurotrophic factor (BDNF) and activation of its high affinity receptor tropomyosin kinase (Trk) B promote retinal ganglion cells (RGCs) survival following injury. In this study, we tested the effects of LM22A-4, a small molecule TrkB receptor-specific partial agonist, on RGC survival *in vitro* and in experimental nonarteritic anterior ischemic optic neuropathy (AION), the most common acute optic neuropathy in those older than 50 years old.

METHODS: We assessed drug effects on immunopanned, cultured RGCs and calculated RGC survival and assessed TrkB receptor activation by mitogen-activated protein (MAP) kinase translocation. To assess effects *in vivo*, we induced murine AION and treated the animals with one intravitreal injection and three-week systemic treatment. We measured drug effects using serial spectral-domain optical coherence tomography (OCT) and quantified retinal $Brn3A^+$ RGC density three weeks after ischemia.

RESULTS: In vitro, LM22A-4 significantly increased the survival of cultured RGCs at day 2 (95% CI control: 8.4–13.6; LM22A-4: 23.7–30.3; BDNF: 24.3–29.9; $P < 0.0001$), similar to the effect of the endogenous TrkB receptor ligand BDNF. There was also significant nuclear and cytoplasmic translocation of MAP kinase (95% CI control: 0.9–6.8; LM22A-4: 38.8–84.4; BDNF: 64.0–93.0; $P = 0.0002$), a known downstream event of TrkB receptor activation. Following AION, LM22A-4 treatment led to significant preservation of the ganglion cell complex (95% CI: AION-PBS: 66.8–70.7%; AION-LM22A-4: 70.0–73.1; $P = 0.03$) and total retinal thickness (95% CI: AION-PBS: 185–196%; AION-LM22A-4: 195–203; $P = 0.002$) as measured by OCT compared with non-treated eyes. There was also significant rescue of the $Brn3A^+$ RGC density on morphometric analysis of whole mount retinae (95% CI control: 2360–2629; AION-PBS: 1647–2008 cells/mm^2; AION-LM22A-4: 1958–2216 cells/mm^2; $P = 0.02$).

*Dr. Barres unfortunately passed away during the preparation of this manuscript. We are grateful for his valuable contribution to all the experiments and the original submitted manuscript.

Correspondence: Y. Joyce Liao, M.D., Ph.D., Associate Professor, Department of Ophthalmology, 2452 Watson Court, Palo Alto, CA 94303-5353, yjliao@stanford.edu, Phone 650-723-6995, Fax 650-725-6619.

Conflict of Interest: Authors declare no conflict of interest.

CONCLUSIONS: TrkB receptor partial agonist LM22A-4 promoted survival of cultured RGCs *in vivo* by TrkB receptor activation, and treatment also led to increased survival of RGCs after optic nerve ischemia, providing support that LM22A-4 may be effective therapy to treat ischemic optic neuropathy.

Keywords

AION; BDNF; TrkB; OCT; retinal ganglion cell; optic neuropathy; pharmacophore

Introduction

Neuronal survival depends on neurotrophins and their receptors, so activation of neurotrophin receptors has been postulated as a way to treat central nervous system neuronal loss. During development and in optic neuropathies, brain-derived neurotrophic factor (BDNF) is the key neurotrophin for retinal ganglion cell (RGC) survival. [1–5] BDNF binds to high affinity tropomyosin-related kinase B (TrkB) receptor, leading to activation of downstream signaling molecules such as mitogen-activated protein (MAP) kinase and phosphatidylinositol 3 (PI3) pathways.[6] Exogenous BDNF as potential neuroprotective treatment has been extensively tested as repeated intravitreal injections of purified protein, topical administration, slowly released in micro-reservoirs, or via gene or cell-based therapies.[3,4] Another way to activate the endogenous neurotrophin pathways is using monoclonal antibodies that directly bind to TrkB receptor. Monoclonal antibodies against TrkB receptor induce phosphorylation of TrkB receptor, activate ERK1/2 and AKT, and are partially effective in rescuing RGCs in experimental glaucoma and optic nerve transection.[7,8]

Since exogenous BDNF or monoclonal antibody agonists as therapeutic agents have potential limitations such as poor blood-brain-barrier penetration, infection, inflammation,[9,10] we became interested in the utility of LM22A-4, ((N,N',N'-tris [2-hydroxyethyl])-1,3,5-benzene tricarbox- amide), which is a small molecule designed to mimic the loop II domain of BDNF and binds selectively to the TrkB receptors.[11] LM22A-4 exhibits specificity and nanomolar affinity for the TrkB receptor and has been shown to increase survival of transfected cells and cultured hippocampal neurons by 56%.[11] LM22A-4 activates TrkB receptor and downstream molecules, AKT and ERK1/2 in cultured hippocampal neurons.[11] The effectiveness of the LM22A-4 has been tested in stroke,[3] spinal cord injury,[12] epilepsy,[13] and neurodegenerative diseases such as Rett syndrome[14,15] and Huntington's disease.[16] In a mouse model of stroke, Han et al. show that the administration of the LM22A-4 three days after ischemia results in phosphorylation of downstream target, AKT and ERK1/2, and improved limb swing speed and gait after stroke.[3]

Among all LM22A compounds, LM22A-4 has been particularly studied due to its selectivity[11,16] for TrkB receptor. Simon *et al.* demonstrated that LM22A-4 and BDNF compete for the TrkB receptor binding without any detectable effects on TrkA and TrkC, or $P75^{NTR}$.[16] Massa *et al.* showed that LM22A-4's specific affinity for TrkB and the absence of $P75^{NTR}$ binding make LM22A-4 distinct from a BDNF mimetic that would have evoked a full range of BDNF-related activities.[11] LM22A-4 can penetrate the blood-brain barrier

in sufficient amount and activates TrkB to initiate cytoplasmic MAPK signaling pathway.[11] Co-administration of TrkB and BDNF leads to a 10%–20% reduction in BDNF activity and no additive effect on survival of hippocampal neurons, consistent with competition for the same TrkB receptor.[11] Application of K252a, a known Trk inhibitor, or an inhibitory antibody that binds to the extracellular domain of TrkB lead to a reduction in neurotrophic activity or increased TUNEL-positive cells of BDNF and LM22A-4.[11]

Anterior ischemic optic neuropathy (AION) is the most common acute optic neuropathy in patients older than 50 years old and often leads to debilitating and permanent (irreversible) loss of vision.[17,18] It is of two types: arteritic and nonarteritic. Retrogradely transported neurotrophins like BDNF are disrupted in optic neuropathies localized to the optic nerve head such as glaucoma,[2] and interruption of axonal transport is found in primate model of nonarteritic AION[19] and is thought to be part of the pathogenesis of nonarteritic AION and optic atrophy.[20] We and others have studied nonarteritic AION model in rodents, using both in vivo imaging and histologic methods.[21–28] Based on the importance of TrkB receptor activation on RGC survival and the potential effects of LM22A-4 on salvaging neurons after ischemic insult, in this study, we tested the effects of LM22A-4 on cultured RGCs and in a photochemical thrombosis model of AION.

Materials and Methods

Animals

Adult wild-type C57BL/6 mice (Charles River, Hollister, CA) were kept at constant temperature, with a 12-hour light/dark cycle, with food and water available at libitum. All animal care and experiments were performed in accordance with the ARVO Guide to Use of Animals in Ophthalmic and Vision Research and with approval from the Stanford University Administrative Panel on Laboratory Animal Care. All procedures were performed under sedation, achieved with intramuscular injection of ketamine 50–100 mg/kg (Hospira Inc., Lake Forest, IL), xylazine 2–5 mg/kg (Bedford Laboratories, Bedford, OH), and buprenorphine 0.05 mg/kg (Bedford Laboratories, Bedford, OH). The pupils of anesthetized mice were pharmacologically dilated with 1% tropicamide (Alcon Laboratories Inc., Fort Worth, TX) and 2.5% phenylephrine hydrochloride (Akorn Inc., Lake Forest, IL).

RGC Culture and Immunopanning

We used primary culture of rat RGC using immunopanning.[6,29,30] We dissected postnatal day 8 retinae from Sprague-Dawley rats (Charles River, Hollister, CA) and dissociated enzymatically to make a suspension of single cells. The panning plates were prepared as described. [29,30] The dissociated retinal cells were incubated in rabbit anti-rat-macrophage antiserum (1:100, Accurate, Westbury, NY), then over the goat-anti-rabbit IgG panning plate to remove nonspecific binding, and over the T11D7 (anti-Thy-1) panning plate to isolate the RGCs after extensive washing. Purified RGCs visually confirmed under microscope and replated after trypsin (GIBCO, Grand Island, NY) dissociation on poly-D-lysine (10 μg/ml, 135 kD, Sigma Aldrich, Saint Louis, MO) and laminin (500X stock, 10μl in 5 ml of Neurobasal, 1 μg/ml; Invitrogen, Carlsbad, CA) coated coverslips. The RGCs were cultured in neurobasal serum-free medium containing DMEM Sato medium.[6,30]

RGCs were immunostained using 1:500–1000 anti-β-tubulin monoclonal antibody (1:500, Covance, Cambridge, MA) and A-488-conjugated goat anti-mouse polyclonal antibody (1:200 dilution, Santa Cruz Biotechnology, Santa Cruz, CA) and DAPI stain (Vectashield, Vector Labs, Burlingame, CA) to visualize the purified RGC and their processes (Fig. 1).

RGC Survival Assay

For survival assay, the RGCs were cultured at 15,000 cells per well on poly-D-lysine and laminin coated coverslips in serum-free Sato media containing NAC (Sigma), BSA (Sigma), penicillin/streptomycin (Gibco), sodium pyruvate (1mM, Gibco), L-glutamine (1 mM, Gibco), triiodothyronine(Sigma), and thyroxine (Sigma). [23] CNTF, BDNF, insulin, and B27 were absent, and 5 μg/mL forskolin was included in all conditions to promote cAMP activation. Negative control included forskolin (5 nM) alone, positive control included BDNF (20 ng/mL), and LM22A-4 (1 μM). The media was changed once about 12 hours after plating. On day-2, the RGCs were fixed with 4% paraformaldehyde in PBS and the live-dead assay was performed using calcein-AM (1:1000, 0.5 μM) and ethidium bromide (1:500, 1 μM) of a live/dead cell assay kit (Invitrogen, Carlsbad, CA). The calcein-AM labeled the live cells (green), while the ethidium bromide labeled dead cells with disrupted membrane. The cells were imaged with 4 and 10x objectives and photographed and counted manually under masked condition with an inverted Nikon Eclipse TS100 microscope (Nikon Instruments, Melville, NY) using 20x objective. The percentage of surviving RGCs was calculated as the number of live cells ($calcein^+$) divided by the number of live and dead ethidium $bromide^+$ cells. Multiple coverslips in multiple experiments were counted and the data pooled to calculate to determine statistical significance using unpaired Student's t-test and Mann-Whitney U test.

MAP Kinase Translocation

On day-2 of RGC culture, we looked for evidence of TrkB receptor activation by looking for MAP kinase translocation.[30] The RGCs were fixed in 4% paraformaldehyde, permeabilized in 0.1% Triton-X 100, blocked with 10% normal goat serum, and then incubated with primary anti-MAP kinase mouse monoclonal antibody (1:200; Millipore, Billerica, MA) and goat anti-rabbit-A568 secondary antibody (1:200, Invitrogen, Carlsbad, CA) and mounted in DAPI-containing Vectashield (Vector Labs). Imaging was performed with an inverted Nikon Eclipse TS100 microscope (Nikon Instruments, Melville, NY) using 4x, 10x, and 20x objectives. Confocal microscopy was also performed. The photographs were quantified in a masked fashion to determine the number of cells that had diffuse or punctate MAP kinase distribution in all conditions to calculate the percentage of each type. We calculated statistical significance using unpaired Student's t-test and Mann-Whitney test.

Photochemical Thrombosis Model of Anterior Ischemic Optic Neuropathy

To assess in vivo effects of LM22A-4, we induced optic nerve head ischemia following intravenous tail vein injection of rose bengal (1.25 mM in 150 μl of phosphate-buffered saline (PBS), Sigma-Aldrich, St. Louis, MO) using a frequency doubled Nd:YAG laser (400 μm diameter, 50mW, 1 second duration, 15 spots, Pascal, OptiMedica, Santa Clara, CA) as a source of focused, low intensity light.[24,26,31] Photoactivation of intravascular rose bengal, a derivative of fluorescein dye, leads to platelet aggregation and selectively damages

vascular endothelium, producing thrombosis while sparing nonvascular tissues.[4,21,28,32,33] Immediately following AION, we saw narrowing of the peripapillary vessels and visible whitening of the optic disc as a result of induced ischemia. Our photochemical thrombosis model created loss of blood supply in the small capillaries surrounding the optic nerve head but not the central artery or vein, which is the case with retinal ischemia. In each animal, AION was induced in one eye and the contralateral eye served as a control.

In Vivo LM22A-4 Treatment

Within hours following optic nerve head ischemia, we treated one eye of each animal with an intravitreal injection of LM22A (5 μg/1 μl in PBS) by 30-gauge Hamilton syringe (Hamilton, Nevada, USA) to deliver the drug intravitreally to the retina and the contralateral eyes were injected with 1 μl PBS alone. Immediately after AION induction, we also started three-week daily on Mondays-Friday systemic (intranasal 50 ng/10 μl and intraperitoneal 1000 μg/200 μl in PBS) treatment to maximize the drug retention and efficiency. The dose, mode and the frequency of the drug administration was chosen based on previous reports.[11,16]

Spectral-Domain OCT Imaging and Analysis

To measure in vivo effects, we performed spectral-domain optical coherence tomography (OCT) analysis using Spectralis™ HRA+OCT instrument (Heidelberg Engineering, GmbH, Heidelberg, Germany), which utilizes a superluminescent diode laser with average wavelength of 870 nm. The OCT scanner has optical axial resolution of 7 μm, digital resolution of 3.5 μm, scan depth of 1.8 mm, and scan rate of 40 kHz. We used the standard objective with a 30° field of view. To correct for the optics of the small mouse eye, we mounted an additional digital high magnification lens (Volk Optical, Inc., Mentor, OH 44060, U.S.A.) in front of the scanning system, similar to other OCT studies of rodent eyes.[34,35] The OCT measurements have been shown to be comparable with that of histology.[24,36] For imaging of the human eyes, OCT measurements assume emmetropia and average axial length, and adjustment for non-human primate has been published.[37] In our mouse study, we assumed there was no significant difference in the refraction, axial length, astigmatism, or optical aberrations in the mouse eyes in different age groups measured under ketamine-xylazine anesthesia.

All animals were measured rapidly following anesthesia and pupillary dilatation. We applied lubricating eye drops over the mouse eyes and covered them with custom-made contact lenses to prevent ocular surface issues. For imaging, animals were placed on an adjustable platform, and the camera was aligned perpendicular to the animal directly in front and very close to the eye using a three-dimensional micromanipulator.[34–36] Once the optic disc was centered and in focus using infrared imaging, we performed the *circular scan* (scan angle 12°, also known as the RNFL scan) (Fig. 3A) using the enhanced depth imaging (EDI) and high-resolution mode, with each B-scan consisting of 1536 A-scans centered around the optic disc. We averaged 16 frames per B-scan.

We also performed *posterior pole scans* (scan angle 30° x 25°) (Fig. 3B) using EDI at high speed mode, with each 2D B-scan consisting of 768 A-scans, average 9 frames per B-scan;

and *25-line scans* (scan angle 25° x 15°) at high resolution mode, average 16 frames per B-scan. Only images with adequate signal strength index were saved and used for analysis. All OCT scans were performed by one investigator to maximize consistency, and the best image from each eye was selected for segmentation.

For the *circular RNFL scans*, we manually segmented the thickness of the ganglion cell complex (GCC),[38,39] which was defined as the combined thickness of the nerve fiber layer, ganglion cell layer, and the inner plexiform layer. We used the G or global measurement of GCC thickness, which is the average of all measurements (360°) around the optic disc. The GCC measurement did not include the outer retina and were not affected by outer retinal ischemia or distortion of the outer nuclear layer due to swelling. Because of the subjective nature of the manual segmentation of the GCC, every effort was made to standardize the segmentation process. The segmentation was performed under magnification and was easily and visually distinguished from the adjacent vitreous on one side and the inner nuclear layer on the other side due to obvious change in signal intensities. The segmentation was performed by one well-trained investigator to reduce variability between investigators, and this person was masked to the identity of the eyes. The segmentation was then visually confirmed by a second investigator as needed. We tested the reliability of manual segmentation in a small number of animals, either by re-imaging the same eyes and segmenting them under masked condition or take the same OCT images and segmenting them several times independently. The R^2 was 0.92 for re-imaging and segmentation of the same eyes on different dates, and the R^2 was 0.85–0.93 for re-segmentation of the same OCT images. Based on these values, we were confident of the consistency of the process.

For the *posterior pole scans*, the total retinal thickness, which was defined as the inner limiting membrane to the Bruch's membrane, was automatically segmented by the Spectralis software and visually confirmed to correct for poor segmentation as needed. Following posterior pole scan, the coronal view of the retina was displayed to show total retinal thickness in a grid composed of 3 × 3 squares, of which the center 2 × 2 grid was averaged to obtain the *optic disc* thickness and the 6 × 6 grid minus the center 2 × 2 grid was used for calculation of *retinal* thickness (Fig. 3B).

Following sedation and pupillary dilatation, we applied lubricating eye drops over the mouse eyes and cover them with custom-made contact lenses to prevent dehydration. Animals were placed on an adjustable platform and aligned with the OCT probe. We measured data at different time points (baseline, day 1, week 1, 2, and 3) using circular scan (12° diameter), the posterior pole analysis (30°x 25° volume scan), and 25-line scan (25°x15°) at high resolution to monitor the retinal thickness around the disc, all enhanced depth imaging (EDI) and high resolution or high speed modes. The circular scan (12°, also known as the retinal nerve fiber layer or RNFL scan) consisted of 1536 A-scans centered at the optic disc with scan rate 19 Hz and average 16 frames per B-scan. The posterior pole scan (30° x 25° volume scan) was average of 9 frames per B-scan, and the 25-line scan (25° x 15°) was average of 16 frames per B-scan. Only images with adequate signal strength index and the clearest layer distinction were analyzed under masked condition.

For the ring analysis, we manually segmented the thickness of the ganglion cell complex (GCC), which was the combination of retinal nerve fiber layer, ganglion cell layer, and inner plexiform layers (RNFL/GCL/IPL), since the retinal nerve fiber layer (axons of retinal ganglion cells) is technically difficult to image reliably after injury. For the posterior pole and 25-line scans, we used automatic segmentation to measure the total retinal thickness around the optic disc using the innermost circle or the central 2 × 2 grid, which were centered on the optic disc. All segmentation images were visually confirmed to ensure accurate measurements of the retinal layers. Statistical analyses were performed using Wilcoxon signed-rank test or Mann-Whitney within the same experimental group or across groups, respectively.

Quantification of Brn3A$^+$ RGCs in Whole Mount Retinae

Following dissection and intracardiac perfusion with 4% paraformaldehyde in PBS, we prepared whole mount retinae per usual protocol and performed immunostaining with anti-Brn3 antibody to stain for RGCs. Briefly, the retinae were permeabilized in PBS 0.5% Triton-containing Tris-buffered saline, blocked with 10% normal goat serum, washed, and incubated overnight at 4°C with goat-anti-Brn3a polyclonal antibody (1:100, Santa Cruz Biotechnology, Santa Cruz, CA) and donkey anti-goat IgG-A488 secondary antibody (1:200, Santa Cruz Biotechnology, Santa Cruz, CA), and mounted in DAPI-containing Vectashield (Vector Labs, Burlingame, CA). We imaged the retinae using an inverted Nikon Eclipse TS100 microscope (Nikon Instruments, Melville, NY) and Metamorph imaging software (Molecular Devices, Sunnyvale, CA). For quantification, 4 images from each of 4 quadrants were used. The RGCs in each image were counted automatically using a program in ImageJ Macro (U.S. National Institutes of Health, Bethesda, Maryland), and each image was then manually reviewed under masked condition for quality of cell count and the results were highly correlated with the automatic count (Fig. 4C). We calculated statistical significance using Mann-Whitney U test.

Statistical Analysis

Data were analysed with commercial statistical software Prism (GraphPad Inc., La Jolla, CA) and Microsoft Office Excel (Richmond, WA). Mann-Whitney U test and Wilcoxon signed-rank test were used to calculate statistical significance, which was defined as $p < 0.05$. All data are presented as mean ± S.E.M.

Results

LM22A-4 promoted RGC survival

Using primary RGC culture following immunopanning,[6] we found that LM22A-4 treatment *in vitro* for 2 days significantly increased RGC survival (negative control: 11.0 ± 1.2%, LM22A-4: 27.0 ± 1.5%, $P < 0.0001$), similar to the effects of the endogenous TrkB receptor ligand, BDNF (27.1 ± 1.2%, $P < 0.0001$ compared with negative control). (Fig. 1)

LM22A-4 induced nuclear localization of MAP kinase in cultured RGCs, consistent with TrkB receptor activation

We assayed MAP kinase nuclear translocation as a global measure of subcellular response of MAPK activation following TrkB receptor activation.[6,30] After 2 days of LM22A-4 exposure, MAP kinase distribution was transformed from a diffuse pattern found in the soma, dendrites, and axons seen in negative control to a punctate pattern that overlaps with that of the nucleus (Fig. 2), consistent with evidence of MAP kinase activation.[6] Although the most intense signal was center near the nuclei, there was also some, punctate anti-MAP kinase staining along the RGC processes (Fig. 2B). This change in MAP kinase distribution was significant compared with negative control ($P = 0.0002$) and similar to the pattern seen with BDNF treatment (Fig. 2C). Taken together with prior studies, which showed high affinity, specific binding of LM22A-4 to TrkB receptor and activation of molecules downstream of TrkB such as ERK, AKT etc. in hippocampal cells and similarity in the physiological response between RGCs and hippocampal cells,[11] our data indicated LM22A-4 improved survival of RGC in culture and suggested that this may be achieved in the setting of TrkB receptor activation.

In vivo effects of LM22A-4 in murine experimental anterior ischemic optic neuropathy

We tested the in vivo effects of LM22A-4 treatment on experimental nonarteritic AION using laser-assisted photochemical thrombosis in one eye of each mouse. Immediately following optic nerve head ischemia, we performed one intravitreal injection into AION and contralateral, control eyes and commenced daily, systemic treatment for 3 weeks using LM22A-4 in PBS or PBS alone (Methods). Briefly, we monitor the in vivo effects of treatment using serial spectral-domain optical coherence tomography (OCT). We measured the thickness of retinal layers that reflect optic nerve anatomy using two methods (Fig. 3): 1) circular scan and manual segmentation of the ganglion cell complex (“GCC”), which is defined as the combined thickness of the retinal nerve fiber layer, ganglion cell layer, and the inner plexiform layer (RNFL/GCL/IPL)[24] and 2) volume scan and automatic segmentation of the total retinal thickness (“TRT”) (retinal nerve fiber layer to retinal pigment epithelium) in the optic disc area.

Three-weeks after AION and treatment, there was a significant preservation of the GCC in the LM22A-4-treated AION eyes compared with PBS-treated AION eyes (AION-PBS: 68.7 ± 0.9 μm, $N = 23$ eyes; AION LM22A-4: 71.6 ± 0.8 μm; $N = 32$ eyes; $P = 0.03$) (Fig. 3A). This 2.9 μm preservation of GCC after LM22A-4 treatment was partial, with significant overall thinning of the GCC regardless of treatment. There was a 7.5 μm thinning after AION in the PBS-treated eyes compared with control eyes (control-PBS: 76.2 ± 1.0, $N = 23$; AION-PBS: 68.7 ± 0.9 μm, $N = 23$; $P < 0.0001$) and a 5.9 μm thinning after AION in the LM22A-4 treated AION eyes compared with LM22A-4-treated control eyes (control-LM22A-4: 77.5 ± 0.6 μm, $N = 31$; AION-LM22A-4: 71.6 ± 0.8 μm, $N = 32$; $P < 0.0001$).

Similar to the significant benefit of LM22A-4 seen on GCC measurements, there was a partial, significant preservation of the TRT of the optic disc area using the posterior pole scans (Fig. 3B). In the LM22A-4-treated AION eyes compared with PBS-treated AION

eyes, the optic disc TRT was significantly preserved by 8.4 μm (AION-PBS: 190.5 ± 2.8 μm, N = 47; AION-LM22A-4: 198.9 ± 1.9 μm, N = 46; P = 0.002). This preservation due to LM22A-4 treatment was partial, since there was significant thinning after AION regardless of treatment. In the PBS-treated group, there was 45.3 μm thinning after AION (control-PBS: 235.8 ± 2.8 μm, N = 41; AION-PBS: 190.5 ± 2.8 μm, N = 47; P < 0.0001). In the LM22A-4-treated group, there was 38.5 μm thinning after AION (control-LM22A-4: 237.4 ± 2.2 μm, N = 51; AION-LM22A-4: 198.9 ± 1.9 μm, N = 46; P < 0.0001). Taken together, the GCC and the optic disc measurements using posterior pole both indicated that LM22A-4 treatment partially preserved retinal thickness after AION. We did not investigate whether LM22A-4 treatment can protect the thickness of ONL/OPL since this is less clinically relevant to human AION. Similarly, we don't not know to what extent experimental AION affects ONL/OPL. Patients suffering from AION demonstrates changes in the outer retina. Moreover, there are reports of loss of amacrine cells after murine AION, which contributes to ONL/IPL. However, AION creates clots in the smaller arterioles surrounding the optic nerve axons, which are the extensions of RGCs, we don't expect to see damage in other layers of the retina apart from GCL.

Increased RGC survival after LM22A-4 treatment

To assess RGC survival following in vivo treatment of LM22A-4 after AION, we performed retinal whole mount preparation and quantified of RGC numbers using immunohistochemistry with Brn3A antibody, which has been well described to label a large population of RGCs.[6,40] In this model, the AION eyes had patches of retinae that were relatively devoid of Brn3A staining. However, we focused the quantification of both the areas of relatively dense Brn3A-staining as well patchy areas. (see Methods). Three-weeks following AION, the LM22A-4-treated group showed significant preservation of $Brn3A^+$ cells in the RGC layer (Fig. 4). LM22A-4 treatment salvaged 254 $Brn3A^+$ cells/mm^2 (AION-PBS: 1837 ± 87 $Brn3A^+$ cells/mm^2, N = 55; AION-LM22A-4: 2091 ± 62 $Brn3A^+$ cells/mm^2, N = 104; P = 0.02). Consistent with the OCT data, the improved RGC survival was partial, with loss of 373 $Brn3A^+$ cells/mm^2 (16%) despite LM22A-4 treatment in the AION eyes (P = 0.0002) and loss of 805 $Brn3A^+$ cells/mm^2 (33%) in the PPBS-treated AION eyes (P < 0.0001).

Discussion

We showed for the first time that a small molecule LM22A-4, which binds to neuronal TrkB receptor with high affinity,[11] promoted the survival of cultured RGC in the setting of TrkB receptor and downstream molecule MAP kinase activation, as seen by nuclear translocation of MAP kinase in a pattern that was similar to the effects of BDNF. *In vivo*, single intravitreal and systemic LM22A-4 administration led to significant preservation of the ganglion cell complex in spectral-domain OCT and $Brn3A^+$ RGCs 3-weeks after experimental anterior ischemic optic neuropathy (AION).

Our data using LM22A-4 to activate TrkB receptor and promote RGC survival are consistent with the well-published idea that BDNF and its high affinity receptor TrkB are critical for RGC survival during development,[1] in adult RGCs,[41,42] and in experimental

optic neuropathies.[43–47] As an endogenous promoter of survival, BDNF increases acutely following optic nerve axonal injury,[48–51] and neurotrophin deprivation is thought to be an important trigger for RGC apoptosis[3,52] and glaucomatous degeneration.[53,54] Initial testing using exogenous BDNF as treatment is promising, and intravitreal BDNF protein injections or viral-mediated BDNF expression promote RGC survival after optic nerve transection or crush and ocular hypertension.[3] However, BDNF may selective preserve the soma but not the axons.[55,56] There is also evidence that BDNF delays but does not prevent the onset of RGC death, despite repeated injections or viral gene delivery.[43,57–59] Issues relating to the full benefit of BDNF include important pathways for axonal and somatic survival unrelated to neurotrophins, such as the inhibitory effects of central myelin on axonal regrowth, and down regulation of TrkB receptors,[6,60] which diminish the effect of BDNF.

Our data suggest that directly activating the TrkB receptor with a small molecule may be a viable therapeutic approach. This approach has been utilized via the use of TrkB receptor activating monoclonal antibodies. Hu *et al.* show that antibody (29D7) mediated activation of the TrkB receptor leads to RGC survival [8,61] and promotes the neurite growth after axotomy. They concluded that 29D7 strongly enhanced RGC survival in culture in a dose-dependent manner, and this effect was augmented by cAMP elevation, which was similar to the activity of cAMP to enhance the RGC response to BDNF for axonal survival and growth.[61–63] Bai *et al.* showed mAb 1D7 recognizes a stable epitope within the D2-D3 ectodomains of the TrkB in the axotomized retina.[8] Both BDNF and mAb 1D7 induce pTyr-TrkB; however, only mAb 1D7 can protect and significantly delay the degeneration of RGCs in the acute and chronic retinal injury *in vivo* by activating TrkB resulting in long-lived physiological effect. Treatment via direct activation of TrkB may have benefits different from that of BDNF application, since BDNF not only binds to high affinity TrkB receptor but also known to bind to p75 receptor, which may have negative impact on survival.[8] BDNF binding to TrkB receptors induces “prosurvival” signals, whereas binding to p75 neurotrophin receptor ($p75^{NTR}$) generally mediates apoptotic signals depending on biological context.[62] This may explain why BDNF only delays but not prevent cell death.[64] This means direct activation of the TrkB receptor using a drug like LM22A-4 may hold promise for future neuroprotective therapy.

There are different potential mechanisms why LM22A-4 effect on experimental AION was partial. 1) The effects of ischemia may be irreversible. 2) TrkB activation is only part of the pathway and its activation only partially rescues the cell death. Bai *et al.* examined the effect of TrkB agonist in a glaucoma rat model and showed that a selective TrkB agonist caused long-lived TrkB activation and significantly delayed RGC death in the acute and chronic retinal injury *in vivo*. Additionally, they showed that TrkB activation preserved retinal structure and provided more efficient neuroprotection.[8] 3) TrkB receptor was not sufficiently localized to the plasma membrane for LM22A-4 binding. There is some in vitro evidence in cultured RGCs that the TrkB receptor becomes internalized, which leads to the loss of trophic responsiveness after axotomy. [6,60] Activation of cAMP has been shown to be important to promote membrane localization of TrkB receptor, so addition of cAMP analog like CpT to LM22A-4 may have synergic effect *in vivo*.[8] Almasieh *et al.* hypothesize that the level of TrkB expression in RGC varies following injury, which may limit the ability of BDNF to activate molecules downstream of the TrkB receptor.[3,57] *In vivo*, TrkB mRNA

and protein levels are substantially down-regulated in adult RGCs following axotomy.[65,66] These findings suggest that reduced TrkB expression in injured RGCs contributes to their desensitization to exogenous, and possibly endogenous, BDNF.

The ability of LM22A-4 to specifically bind to and activate TrkB receptor has been well shown in transfected cells and hippocampal and other neurons, and this paper provided some evidence in RGCs. The effectiveness of the LM22A-4 has been extensively tested *in vitro* and in models of stroke[67] and neurodegenerative diseases such as Rett syndrome[68,69] and Huntington's disease,[16] Fragile-X syndrome.[70] In the mouse model of stroke, Han *et al.* showed that the administration of the LM22A-4 three days after ischemia resulted in phosphorylation of downstream target, AKT and ERK, and improved limb swing speed and gait after stroke.[67,71] Al-qudah *et al.* demonstrated the effect of LM22A-4 in the rabbit intestinal longitudinal muscle.[72] Kajiya *et al.* demonstrated that LM22A-4 regulates cementoblalst differentiation via TrkB-ERK/AKT signaling cascade.[73] Warnault *et al.* showed that compulsive alcohol drinking can be reversed in mice by TrkB activation such as LM22A-4.[74] Massa *et al.* demonstrated that in hippocampal neurons treated with LM22A-4 *in vitro* reduces amyloid β−induced cell death, attenuates 1-methyl-4-phenylpyridinium (MPP^+)-induced cell death in SH-SY5Y human tumor cell line for Huntington's disease mode.[71] Similarly, a small molecule TrkB agonists have also been used to treat other neurodegenerative diseases. For example, 7,8-DHF mimics the physiological effects of BDNF and has strong therapeutic potential to be used in Parkinson's disease,[75] Huntingtons's disease,[76] amyotrophic lateral sclerosis,[77] and Alzheimer's disease.[78] However, some studies also showed no effects of LM22A-4[79,80] *in vitro*.

Our study demonstrated the translocation of MAPK family members from the perinuclear to the nuclear localization upon neurotrophin treatment. Upon activation, MAPK family members, regulates a large number of stress-induced cellular signaling by transcriptional regulation, chromatin remodeling, cell cycle entry etc. One of its modes of activation is its nuclear translocation. For example, Brunet *et al.* demonstrated that, relocalization of p42/p44 MAPK from cytosol to nucleus is essential for activating its downstream target Elk-1 for mediating mitogen-induced gene expression and cell cycle entry.[81,82] Similarly, neurotrophic factor-mediated MAPK family member such as ERK1/2 activation is required for neuroprotection in CNS neurons[83] as well as RGCs.[61] However, we cannot deny the contribution of pro-apoptotic pathways such as JNK or p38 after neurotrophic factor treatment.[84] Moreover, we have not investigated the individual contribution of each MAPK family members in LM22A-4-mediated neuroprotection, and the details about the contribution of each MAPK family member in LM22A-4 should be further investigated in future experiments. Also, we have not investigated whether MAPK inhibitors can inhibit the survival-promoting effect of LM22A-4 in vitro. However, in human cementoblast-like (HCEM) cell line, use of an MEK-ERK inhibitor (U0126) attenuates pro-survival molecules such as ERK and Akt and TrkB activation.[73] Therefore, it is likely that LM22A-4 might have pro-survival effect by MAPK pathways. Although the similarities between LM22A-4 and BDNF action have been shown, more work is needed to decipher what the differences may be and the potential impact of LM22A-4 as a therapeutic agent.

Limitations to our study include the use of cultured RGCs and MAP kinase translocation rather than *in vivo* method as a method to demonstrate TrkB receptor activation, which is a nice global measure of TrkB receptor activation.[6,30]The impact of TrkB receptor activation in RGCs and after LM22A-4 application *in vivo* should be further investigated in order to better understand the mechanism of its benefit in vitro and in vivo. Although there is good evidence in the cultured RGC system that TrkB receptor agonism synergizes well with application of forskolin through cAMP activation, we chose to only test the effect of LM22A-4 alone *in vivo*. This is because we wanted to investigate the effect of LM22A-4 alone without the confounding neuroprotective effect of forskolin.[85] We anticipate that combined treatment of LM22A-4 and forskolin *in vivo* may yield synergistic or additive benefits for neuroprotection.

In conclusion, treatment for human nonarteritic AION remains extremely limited, and molecules like LM22A-4 may be promising therapy, either alone or in combination with other drugs, in human AION. Although we only tested the benefit of LM22A-4 in a model of nonarteritic AION, we anticipate that this benefit can be generalized to the treatment of arteritic AION, given corticosteroid treatment to dampen the inflammatory aspect of arteritic AION often does not rescue vision, probably because there is no additional neuroprotective effect of corticosteroid treatment. LM22A-4 also has a simple, flexible chemical structure, which is amenable to chemical modifications to increase its therapeutic potential in the future.

Acknowledgment

We thank Gun Ho Lee and Jeffry Ma for their help with experiments.

We thank Ben A. Barres for his great contribution in this manuscript, who is deceased now.

Financial Disclosure:

Y.J.L was supported by the Career Award in Biomedical Sciences from the Burroughs Wellcome Foundation, Western Havens Foundation, and the North American Neuro-Ophthalmology Society Pilot Grant, National Eye Institute (P30-026877), and Research to Prevent Blindness, Inc.

Abbreviations:

AION	anterior ischemic optic neuropathy
BDNF	Brain-derived neurotrophic factor
GCC	ganglion cell complex
MAP	mitogen-activated protein
OCT	spectral-domain optical coherence tomography
OD	right eye
ON	optic nerve
ONH	optic nerve head

OS	left eye
RGC	retinal ganglion cell
Trk	tropomyosin kinase

References:

1. Johnson JE, Barde YA, Schwab M, Thoenen H. 1986. Brain-derived neurotrophic factor supports the survival of cultured rat retinal ganglion cells. J Neurosci. 6(10):3031–3038. [PubMed: 2876066]
2. Burgoyne CF. 2011. A biomechanical paradigm for axonal insult within the optic nerve head in aging and glaucoma. Exp Eye Res. 93(2):120–132. [PubMed: 20849846]
3. Almasieh M, Wilson AM, Morquette B, Cueva Vargas JL, Di Polo A. 2012. The molecular basis of retinal ganglion cell death in glaucoma. Prog Retin Eye Res. 31(2):152–181. [PubMed: 22155051]
4. Bernstein SL, Johnson MA, Miller NR. 2011. Nonarteritic anterior ischemic optic neuropathy (naion) and its experimental models. Prog Retin Eye Res. 30(3):167–187. [PubMed: 21376134]
5. Mysona BA, Zhao J, Bollinger KE. 2017. Role of bdnf/trkb pathway in the visual system: Therapeutic implications for glaucoma. Expert Rev Ophthalmol. 12(1):69–81. [PubMed: 28751923]
6. Meyer-Franke A, Kaplan MR, Pfrieger FW, Barres BA. 1995. Characterization of the signaling interactions that promote the survival and growth of developing retinal ganglion cells in culture. Neuron. 15(4):805–819. [PubMed: 7576630]
7. Acheson J. 2010. Blindness in neurological disease: A short overview of new therapies from translational research. Curr Opin Neurol. 23(1):1–3. [PubMed: 20038826]
8. Bai Y, Xu J, Brahimi F, Zhuo Y, Sarunic MV, Saragovi HU. 2010. An agonistic trkb mab causes sustained trkb activation, delays rgc death, and protects the retinal structure in optic nerve axotomy and in glaucoma. Invest Ophthalmol Vis Sci. 51(9):4722–4731. [PubMed: 20357199]
9. Poduslo JF, Curran GL. 1996. Permeability at the blood-brain and blood-nerve barriers of the neurotrophic factors: Ngf, cntf, nt-3, bdnf. Brain research Molecular brain research. 36(2):280–286. [PubMed: 8965648]
10. Falavarjani KG, Nguyen QD. 2013. Adverse events and complications associated with intravitreal injection of anti-vegf agents: A review of literature. Eye (Lond). 27(7):787–794. [PubMed: 23722722]
11. Bienvenu F, Jirawatnotai S, Elias JE, Meyer CA, Mizeracka K, Marson A, Frampton GM, Cole MF, Odom DT, Odajima J et al. 2010. Transcriptional role of cyclin d1 in development revealed by a genetic-proteomic screen. Nature. 463(7279):374–378. [PubMed: 20090754]
12. Agemy SA, Scripsema NK, Shah CM, Chui T, Garcia PM, Lee JG, Gentile RC, Hsiao YS, Zhou Q, Ko T et al. 2015. Retinal vascular perfusion density mapping using optical coherence tomography angiography in normals and diabetic retinopathy patients. Retina. 35(11):2353–2363. [PubMed: 26465617]
13. Cao D, Yang D, Huang Z, Zeng Y, Wang J, Hu Y, Zhang L. 2018. Optical coherence tomography angiography discerns preclinical diabetic retinopathy in eyes of patients with type 2 diabetes without clinical diabetic retinopathy. Acta diabetologica.
14. Herrmann KH, Schmidt S, Kretz A, Haenold R, Krumbein I, Metzler M, Gaser C, Witte OW, Reichenbach JR. 2012. Possibilities and limitations for high resolution small animal mri on a clinical whole-body 3t scanner. Magma. 25(3):233–244. [PubMed: 22042538]
15. Anegondi N, Chidambara L, Bhanushali D, Gadde SGK, Yadav NK, Sinha Roy A. 2017. An automated framework to quantify areas of regional ischemia in retinal vascular diseases with oct angiography. Journal of biophotonics.
16. Simmons DA, Belichenko NP, Yang T, Condon C, Monbureau M, Shamloo M, Jing D, Massa SM, Longo FM. 2013. A small molecule trkb ligand reduces motor impairment and neuropathology in r6/2 and bachd mouse models of huntington's disease. J Neurosci. 33(48):18712–18727. [PubMed: 24285878]
17. Hayreh SS. 1974. Anterior ischaemic optic neuropathy. Iii. Treatment, prophylaxis, and differential diagnosis. Br J Ophthalmol. 58(12):981–989. [PubMed: 4376417]

18. Arnold AC. 1995. Anterior ischemic optic neuropathy. Semin Ophthalmol. 10(3):221–233. [PubMed: 10159747]
19. McLeod D, Marshall J, Kohner EM. 1980. Role of axoplasmic transport in the pathophysiology of ischaemic disc swelling. Br J Ophthalmol. 64(4):247–261. [PubMed: 6155935]
20. Hayreh SS. 2009. Ischemic optic neuropathy. Prog Retin Eye Res. 28(1):34–62. [PubMed: 19063989]
21. Bernstein SL, Guo Y, Kelman SE, Flower RW, Johnson MA. 2003. Functional and cellular responses in a novel rodent model of anterior ischemic optic neuropathy. Invest Ophthalmol Vis Sci. 44(10):4153–4162. [PubMed: 14507856]
22. Goldenberg-Cohen N, Guo Y, Margolis F, Cohen Y, Miller NR, Bernstein SL. 2005. Oligodendrocyte dysfunction after induction of experimental anterior optic nerve ischemia. Invest Ophthalmol Vis Sci. 46(8):2716–2725. [PubMed: 16043843]
23. Pangratz-Fuehrer S, Kaur K, Ousman SS, Steinman L, Liao YJ. 2011. Functional rescue of experimental ischemic optic neuropathy with alphab-crystallin. Eye (Lond). 25(6):809–817. [PubMed: 21475310]
24. Ardeljan D, Chan CC. 2013. Aging is not a disease: Distinguishing age-related macular degeneration from aging. Prog Retin Eye Res.
25. Lin TP, Adler CH, Hentz JG, Balcer LJ, Galetta SL, Devick S. 2014. Slowing of number naming speed by king-devick test in parkinson's disease. Parkinsonism & related disorders. 20(2):226–229. [PubMed: 24269283]
26. Characteristics of patients with nonarteritic anterior ischemic optic neuropathy eligible for the ischemic optic neuropathy decompression trial. 1996. Arch Ophthalmol. 114(11):1366–1374. [PubMed: 8906027]
27. Shariati MA, Park JH, Liao YJ. 2015. Optical coherence tomography study of retinal changes in normal aging and after ischemia. Invest Ophthalmol Vis Sci. 56(5):2790–2797. [PubMed: 25414186]
28. Bhardwaj S, Tsui E, Zahid S, Young E, Mehta N, Agemy S, Garcia P, Rosen RB, Young JA. 2017. Value of fractal analysis of optical coherence tomography angiography in various stages of diabetic retinopathy. Retina.
29. Huettner JE, Baughman RW. 1986. Primary culture of identified neurons from the visual cortex of postnatal rats. J Neurosci. 6(10):3044–3060. [PubMed: 3760948]
30. Meyer-Franke A, Wilkinson GA, Kruttgen A, Hu M, Munro E, Hanson MG Jr., Reichardt LF, Barres BA. 1998. Depolarization and camp elevation rapidly recruit trkb to the plasma membrane of cns neurons. Neuron. 21(4):681–693. [PubMed: 9808456]
31. Hajian S, Shariati M, Mirzaii Najmabadi K, Yunesian M, Ajami MI. 2015. Use of the extended parallel process model (eppm) to predict iranian women's intention for vaginal delivery. J Transcult Nurs. 26(3):234–243. [PubMed: 24692339]
32. Slater BJ, Mehrabian Z, Guo Y, Hunter A, Bernstein SL. 2008. Rodent anterior ischemic optic neuropathy (raion) induces regional retinal ganglion cell apoptosis with a unique temporal pattern. Invest Ophthalmol Vis Sci. 49(8):3671–3676. [PubMed: 18660428]
33. Azizi P, Golshekan M, Shariati S, Rahchamani J. 2015. Solid phase extraction of cu2+, ni2+, and co2+ ions by a new magnetic nano-composite: Excellent reactivity combined with facile extraction and determination. Environ Monit Assess. 187(4):185. [PubMed: 25784609]
34. Guo L, Normando EM, Nizari S, Lara D, Cordeiro MF. 2010. Tracking longitudinal retinal changes in experimental ocular hypertension using the cslo and spectral domain-oct. Invest Ophthalmol Vis Sci. 51(12):6504–6513. [PubMed: 20688741]
35. Rosch S, Johnen S, Muller F, Pfarrer C, Walter P. 2014. Correlations between erg, oct, and anatomical findings in the rd10 mouse. J Ophthalmol. 2014:874751.
36. Fischer MD, Huber G, Beck SC, Tanimoto N, Muehlfriedel R, Fahl E, Grimm C, Wenzel A, Reme CE, van de Pavert SA et al. 2009. Noninvasive, in vivo assessment of mouse retinal structure using optical coherence tomography. PLoS One. 4(10):e7507. [PubMed: 19838301]
37. Fortune B, Cull GA, Burgoyne CF. 2008. Relative course of retinal nerve fiber layer birefringence and thickness and retinal function changes after optic nerve transection. Invest Ophthalmol Vis Sci. 49(10):4444–4452. [PubMed: 18566463]

38. Nakano N, Ikeda HO, Hangai M, Muraoka Y, Toda Y, Kakizuka A, Yoshimura N. 2011. Longitudinal and simultaneous imaging of retinal ganglion cells and inner retinal layers in a mouse model of glaucoma induced by n-methyl-d-aspartate. Invest Ophthalmol Vis Sci. 52(12):8754–8762. [PubMed: 22003119]
39. Hein K, Gadjanski I, Kretzschmar B, Lange K, Diem R, Sattler MB, Bahr M. 2011. An optical coherence tomography study on degeneration of retinal nerve fiber layer in rats with autoimmune optic neuritis. Invest Ophthalmol Vis Sci. 53(1):157–163.
40. Nadal-Nicolas FM, Jimenez-Lopez M, Sobrado-Calvo P, Nieto-Lopez L, Canovas-Martinez I, Salinas-Navarro M, Vidal-Sanz M, Agudo M. 2009. Brn3a as a marker of retinal ganglion cells: Qualitative and quantitative time course studies in naive and optic nerve-injured retinas. Invest Ophthalmol Vis Sci. 50(8):3860–3868. [PubMed: 19264888]
41. Thanos S, Bahr M, Barde YA, Vanselow J. 1989. Survival and axonal elongation of adult rat retinal ganglion cells. Eur J Neurosci. 1(1):19–26. [PubMed: 12106170]
42. Cohen-Cory S, Fraser SE. 1995. Effects of brain-derived neurotrophic factor on optic axon branching and remodelling in vivo. Nature. 378(6553):192–196. [PubMed: 7477323]
43. Mansour-Robaey S, Clarke DB, Wang YC, Bray GM, Aguayo AJ. 1994. Effects of ocular injury and administration of brain-derived neurotrophic factor on survival and regrowth of axotomized retinal ganglion cells. Proc Natl Acad Sci U S A. 91(5):1632–1636. [PubMed: 8127857]
44. Weber AJ, Viswanathan S, Ramanathan C, Harman CD. 2010. Combined application of bdnf to the eye and brain enhances ganglion cell survival and function in the cat after optic nerve injury. Invest Ophthalmol Vis Sci. 51(1):327–334. [PubMed: 19710411]
45. Liao YJ, Hwang JJ. 2013. Treatment of anterior ischemic optic neuropathy: Clues from the bench. Taiwan Journal of Ophthalmology.
46. Weber AJ, Harman CD. 2008. Bdnf preserves the dendritic morphology of alpha and beta ganglion cells in the cat retina after optic nerve injury. Invest Ophthalmol Vis Sci. 49(6):2456–2463. [PubMed: 18263808]
47. Zhu W, Chen T, Jin L, Wang H, Yao F, Wang C, Wang Q, Congdon N. 2017. Carotid artery intimal medial thickness and carotid artery plaques in hypertensive patients with non-arteritic anterior ischaemic optic neuropathy. Graefes Arch Clin Exp Ophthalmol.
48. Gao H, Hollyfield JG. 1992. Aging of the human retina. Differential loss of neurons and retinal pigment epithelial cells. Invest Ophthalmol Vis Sci. 33(1):1–17. [PubMed: 1730530]
49. Chen G, Gulbranson DR, Hou Z, Bolin JM, Ruotti V, Probasco MD, Smuga-Otto K, Howden SE, Diol NR, Propson NE et al. 2011. Chemically defined conditions for human ipsc derivation and culture. Nat Methods. 8(5):424–429. [PubMed: 21478862]
50. Wang DY, Ray A, Rodgers K, Ergorul C, Hyman BT, Huang W, Grosskreutz CL. 2010. Global gene expression changes in rat retinal ganglion cells in experimental glaucoma. Invest Ophthalmol Vis Sci. 51(8):4084–4095. [PubMed: 20335623]
51. Rudzinski M, Wong TP, Saragovi HU. 2004. Changes in retinal expression of neurotrophins and neurotrophin receptors induced by ocular hypertension. J Neurobiol. 58(3):341–354. [PubMed: 14750147]
52. Pease ME, McKinnon SJ, Quigley HA, Kerrigan-Baumrind LA, Zack DJ. 2000. Obstructed axonal transport of bdnf and its receptor trkb in experimental glaucoma. Invest Ophthalmol Vis Sci. 41(3):764–774. [PubMed: 10711692]
53. Glovinsky Y, Quigley HA, Dunkelberger GR. 1991. Retinal ganglion cell loss is size dependent in experimental glaucoma. Invest Ophthalmol Vis Sci. 32(3):484–491. [PubMed: 2001923]
54. Quigley HA, McKinnon SJ, Zack DJ, Pease ME, Kerrigan-Baumrind LA, Kerrigan DF, Mitchell RS. 2000. Retrograde axonal transport of bdnf in retinal ganglion cells is blocked by acute iop elevation in rats. Invest Ophthalmol Vis Sci. 41(11):3460–3466. [PubMed: 11006239]
55. Pernet V, Di Polo A. 2006. Synergistic action of brain-derived neurotrophic factor and lens injury promotes retinal ganglion cell survival, but leads to optic nerve dystrophy in vivo. Brain. 129(Pt 4):1014–1026. [PubMed: 16418178]
56. Leaver SG, Cui Q, Plant GW, Arulpragasam A, Hisheh S, Verhaagen J, Harvey AR. 2006. Aav-mediated expression of cntf promotes long-term survival and regeneration of adult rat retinal ganglion cells. Gene Ther. 13(18):1328–1341. [PubMed: 16708079]

57. Di Polo A, Aigner LJ, Dunn RJ, Bray GM, Aguayo AJ. 1998. Prolonged delivery of brain-derived neurotrophic factor by adenovirus-infected muller cells temporarily rescues injured retinal ganglion cells. Proc Natl Acad Sci U S A. 95(7):3978–3983. [PubMed: 9520478]
58. Clarke DB, Bray GM, Aguayo AJ. 1998. Prolonged administration of nt-4/5 fails to rescue most axotomized retinal ganglion cells in adult rats. Vision Res. 38(10):1517–1524. [PubMed: 9667016]
59. Chen H, Weber AJ. 2004. Brain-derived neurotrophic factor reduces trkb protein and mrna in the normal retina and following optic nerve crush in adult rats. Brain Res. 1011(1):99–106. [PubMed: 15140649]
60. Shen S, Wiemelt AP, McMorris FA, Barres BA. 1999. Retinal ganglion cells lose trophic responsiveness after axotomy. Neuron. 23(2):285–295. [PubMed: 10399935]
61. Hu Y, Cho S, Goldberg JL. 2010. Neurotrophic effect of a novel trkb agonist on retinal ganglion cells. Invest Ophthalmol Vis Sci. 51(3):1747–1754. [PubMed: 19875669]
62. Chao MV, Bothwell M. 2002. Neurotrophins: To cleave or not to cleave. Neuron. 33(1):9–12. [PubMed: 11779474]
63. Goldberg JL, Espinosa JS, Xu Y, Davidson N, Kovacs GT, Barres BA. 2002. Retinal ganglion cells do not extend axons by default: Promotion by neurotrophic signaling and electrical activity. Neuron. 33(5):689–702. [PubMed: 11879647]
64. Doi D, Morizane A, Kikuchi T, Onoe H, Hayashi T, Kawasaki T, Motono M, Sasai Y, Saiki H, Gomi M et al. 2012. Prolonged maturation culture favors a reduction in the tumorigenicity and the dopaminergic function of human esc-derived neural cells in a primate model of parkinson's disease. Stem Cells. 30(5):935–945. [PubMed: 22328536]
65. Chen H, Weber AJ. 2002. Expression of glial fibrillary acidic protein and glutamine synthetase by muller cells after optic nerve damage and intravitreal application of brain-derived neurotrophic factor. Glia. 38(2):115–125. [PubMed: 11948805]
66. Cui Q, Tang LS, Hu B, So KF, Yip HK. 2002. Expression of trka, trkb, and trkc in injured and regenerating retinal ganglion cells of adult rats. Invest Ophthalmol Vis Sci. 43(6):1954–1964. [PubMed: 12037005]
67. Han J, Pollak J, Yang T, Siddiqui MR, Doyle KP, Taravosh-Lahn K, Cekanaviciute E, Han A, Goodman JZ, Jones B et al. 2012. Delayed administration of a small molecule tropomyosin-related kinase b ligand promotes recovery after hypoxic-ischemic stroke. Stroke; a journal of cerebral circulation. 43(7):1918–1924.
68. Schmid DA, Yang T, Ogier M, Adams I, Mirakhur Y, Wang Q, Massa SM, Longo FM, Katz DM. 2012. A trkb small molecule partial agonist rescues trkb phosphorylation deficits and improves respiratory function in a mouse model of rett syndrome. J Neurosci. 32(5):1803–1810. [PubMed: 22302819]
69. Kron M, Lang M, Adams IT, Sceniak M, Longo F, Katz DM. 2014. A bdnf loop-domain mimetic acutely reverses spontaneous apneas and respiratory abnormalities during behavioral arousal in a mouse model of rett syndrome. Dis Model Mech. 7(9):1047–1055. [PubMed: 25147297]
70. Nomura T, Musial TF, Marshall JJ, Zhu Y, Remmers CL, Xu J, Nicholson DA, Contractor A. 2017. Delayed maturation of fast-spiking interneurons is rectified by activation of the trkb receptor in the mouse model of fragile x syndrome. J Neurosci. 37(47):11298–11310. [PubMed: 29038238]
71. Massa SM, Yang T, Xie Y, Shi J, Bilgen M, Joyce JN, Nehama D, Rajadas J, Longo FM. 2010. Small molecule bdnf mimetics activate trkb signaling and prevent neuronal degeneration in rodents. J Clin Invest. 120(5):1774–1785. [PubMed: 20407211]
72. Al-Qudah M, Anderson CD, Mahavadi S, Bradley ZL, Akbarali HI, Murthy KS, Grider JR. 2014. Brain-derived neurotrophic factor enhances cholinergic contraction of longitudinal muscle of rabbit intestine via activation of phospholipase c. Am J Physiol Gastrointest Liver Physiol. 306(4):G328–337. [PubMed: 24356881]
73. Kajiya M, Takeshita K, Kittaka M, Matsuda S, Ouhara K, Takeda K, Takata T, Kitagawa M, Fujita T, Shiba H et al. 2014. Bdnf mimetic compound lm22a-4 regulates cementoblast differentiation via the trkb-erk/akt signaling cascade. International immunopharmacology.
74. Warnault V, Darcq E, Morisot N, Phamluong K, Wilbrecht L, Massa SM, Longo FM, Ron D. 2016. The bdnf valine 68 to methionine polymorphism increases compulsive alcohol drinking in

mice that is reversed by tropomyosin receptor kinase b activation. Biol Psychiatry. 79(6):463–473. [PubMed: 26204799]

75. Jang SW, Liu X, Yepes M, Shepherd KR, Miller GW, Liu Y, Wilson WD, Xiao G, Blanchi B, Sun YE et al. 2010. A selective trkb agonist with potent neurotrophic activities by 7,8-dihydroxyflavone. Proc Natl Acad Sci U S A. 107(6):2687–2692. [PubMed: 20133810]
76. Jiang M, Peng Q, Liu X, Jin J, Hou Z, Zhang J, Mori S, Ross CA, Ye K, Duan W. 2013. Small-molecule trkb receptor agonists improve motor function and extend survival in a mouse model of huntington's disease. Hum Mol Genet. 22(12):2462–2470. [PubMed: 23446639]
77. Korkmaz OT, Aytan N, Carreras I, Choi JK, Kowall NW, Jenkins BG, Dedeoglu A. 2014. 7,8-dihydroxyflavone improves motor performance and enhances lower motor neuronal survival in a mouse model of amyotrophic lateral sclerosis. Neuroscience letters. 566:286–291. [PubMed: 24637017]
78. Devi L, Ohno M. 2012. 7,8-dihydroxyflavone, a small-molecule trkb agonist, reverses memory deficits and bace1 elevation in a mouse model of alzheimer's disease. Neuropsychopharmacology. 37(2):434–444. [PubMed: 21900882]
79. Todd D, Gowers I, Dowler SJ, Wall MD, McAllister G, Fischer DF, Dijkstra S, Fratantoni SA, van de Bospoort R, Veenman-Koepke J et al. 2014. A monoclonal antibody trkb receptor agonist as a potential therapeutic for huntington's disease. PLoS One. 9(2):e87923.
80. Boltaev U, Meyer Y, Tolibzoda F, Jacques T, Gassaway M, Xu Q, Wagner F, Zhang YL, Palmer M, Holson E et al. 2017. Multiplex quantitative assays indicate a need for reevaluating reported small-molecule trkb agonists. Sci Signal. 10(493).
81. Brunet A, Roux D, Lenormand P, Dowd S, Keyse S, Pouyssegur J. 1999. Nuclear translocation of p42/p44 mitogen-activated protein kinase is required for growth factor-induced gene expression and cell cycle entry. Embo J. 18(3):664–674. [PubMed: 9927426]
82. Chen RH, Sarnecki C, Blenis J. 1992. Nuclear localization and regulation of erk- and rsk-encoded protein kinases. Mol Cell Biol. 12(3):915–927. [PubMed: 1545823]
83. Hetman M, Kanning K, Cavanaugh JE, Xia Z. 1999. Neuroprotection by brain-derived neurotrophic factor is mediated by extracellular signal-regulated kinase and phosphatidylinositol 3-kinase. J Biol Chem. 274(32):22569–22580. [PubMed: 10428835]
84. Kenchappa RS, Tep C, Korade Z, Urra S, Bronfman FC, Yoon SO, Carter BD. 2010. P75 neurotrophin receptor-mediated apoptosis in sympathetic neurons involves a biphasic activation of jnk and up-regulation of tumor necrosis factor-alpha-converting enzyme/adam17. J Biol Chem. 285(26):20358–20368. [PubMed: 20421303]
85. Corredor RG, Trakhtenberg EF, Pita-Thomas W, Jin X, Hu Y, Goldberg JL. 2012. Soluble adenylyl cyclase activity is necessary for retinal ganglion cell survival and axon growth. J Neurosci. 32(22):7734–7744. [PubMed: 22649251]

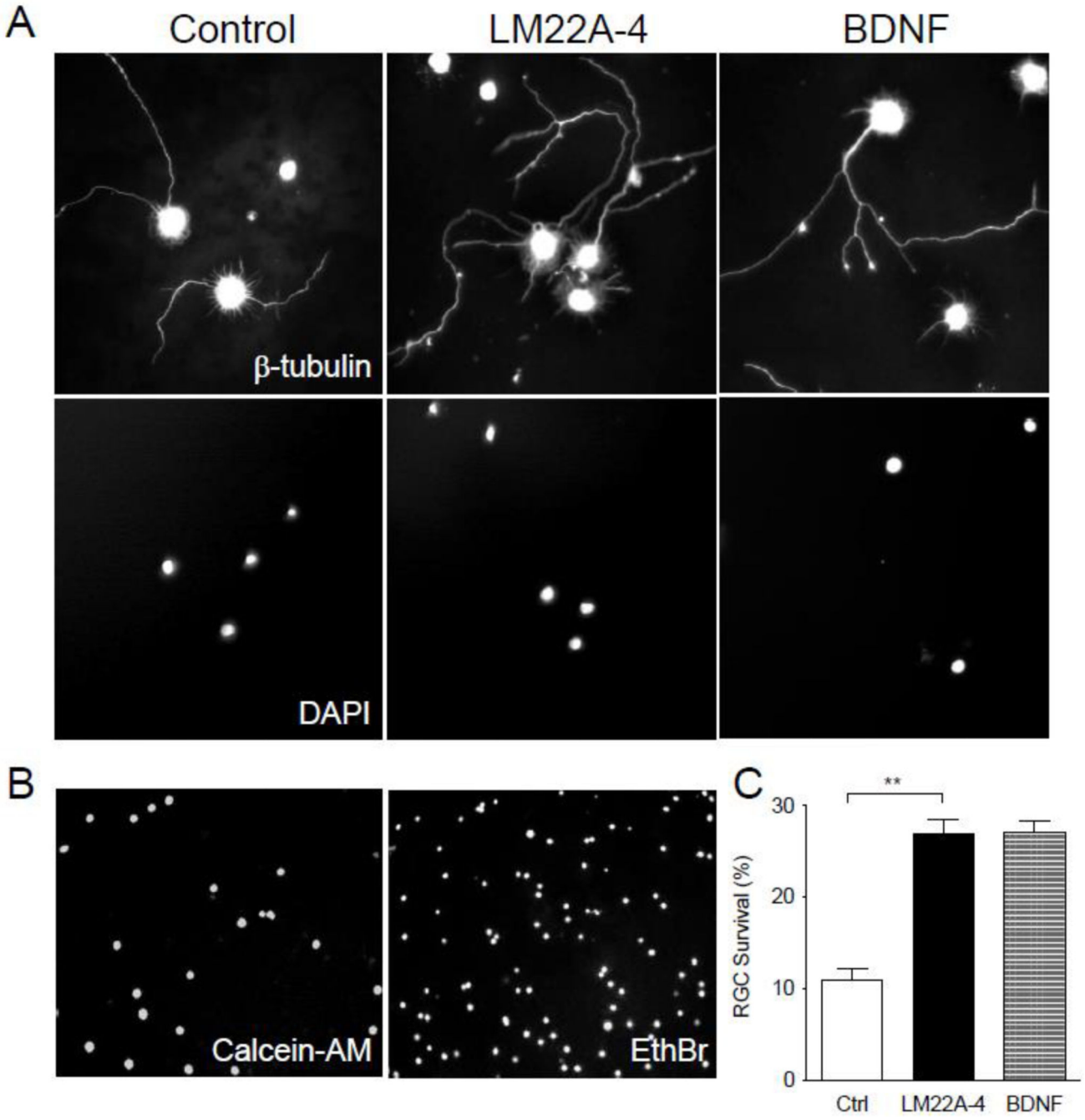

Figure 1.

LM22A-4 treatment increased survival of cultured RGCs on day 2. **(A)** Purified RGCs cultured stained with β-tubulin antibody and DAPI. Many cells exhibited short processes in all conditions. **(B)** Live-dead assay of RGCs using calcein-AM and ethidium bromide to calculate survival. **(C)** Bar graph of survival assay that showed treatment with LM22A-4 significantly increased RGC survival ($P < 0.0001$) similar to the effect of BDNF.

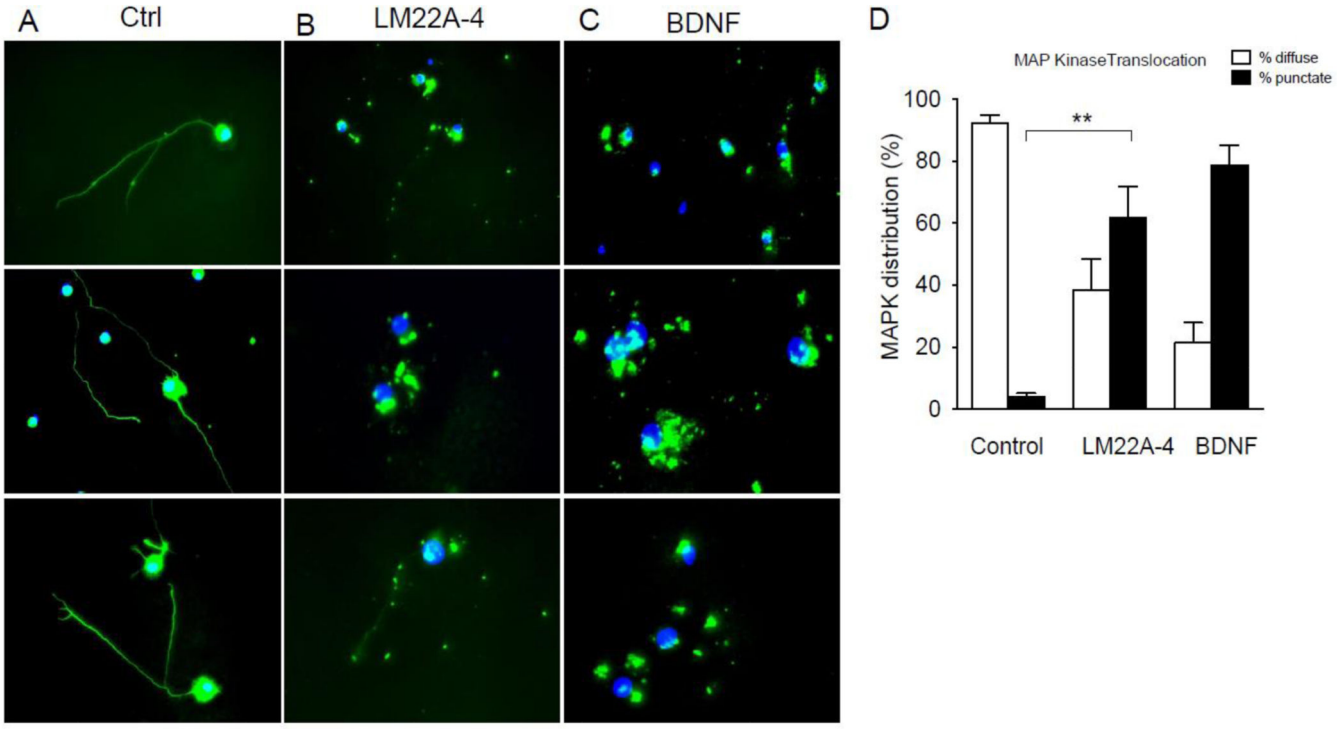

Figure 2.

LM22A-4 treatment promoted TrkB receptor activation and MAP kinase translocation in cultured RGCs on day 2. **(A)** Control. **(B)** LM22A-4 treated. **(C)** BDNF-treated. Top row: lower magnification images. Middle and bottom rows: higher magnification images. **(D)** Bar graph of MAP kinase distribution in a diffuse or punctate, pattern. In control condition in **(A)**, the RGCs exhibited diffuse anti-MAP kinase staining in the soma and processes. In LM22A-4 and BDNF treated groups **(B,C)** there was a significant change in the distribution with punctate appearance of anti-MAP kinase staining in and around the nuclei and decreased and punctate distribution in the neurites.

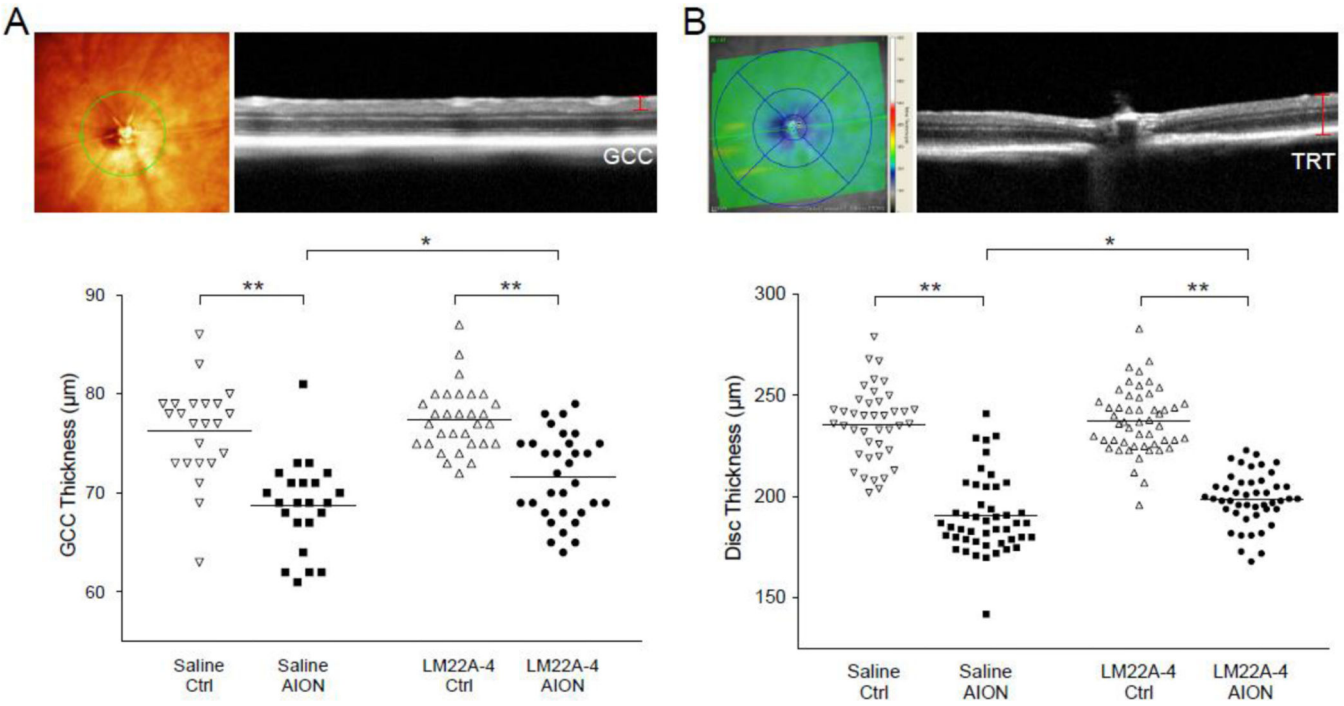

Figure 3.

In vivo treatment with LM22A-4 after experimental AION led to preserved retinal thickness measured using SD-OCT. **(A)** Top: example of fundus photograph and B-scan using the circular scan pattern. Bottom: Bar graph of GCC measurements in different treatment groups showing there was significant preservation of GCC layer thickness in the AION group after three weeks of LM22A-4 treatment (N = 23, P = 0.03). **(B)** Top: example of fundus photograph and B-scan using the posterior pole analysis. TRT: total retinal thickness. Bottom: bar graph of total retinal thickness of the optic disc week-3 after AION showing LM22A-4 treatment significantly improved optic disc thickness (N = 46, P = 0.002). GCC: Ganglion cell layer

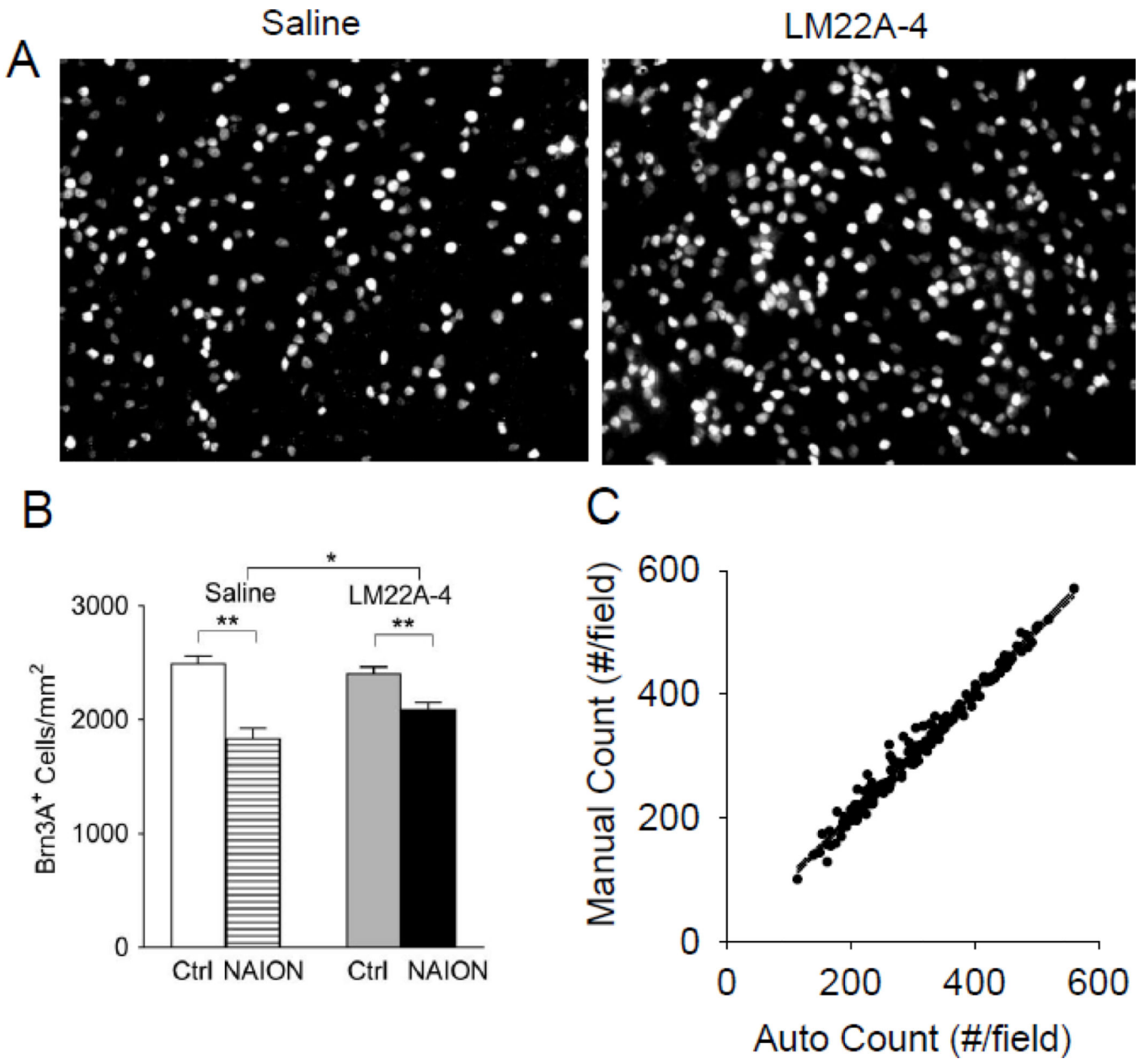

Figure 4.

In vivo LM22A-4 treatment led to increased survival of Brn3A$^+$ RGCs after AION. **(A)** Representative images of Brn3A$^+$ RGCs in PBS-treated and LM22A-4 treated groups at week-3. **(B)** Bar graph of quantification of Brn3A$^+$ cells in control and AION eyes treated with LM22A-4 showing significant increase in Brn3A$^+$ RGCs after LM22A-4 treatment in the AION groups (P = 0.02). **(C)** High correlation of the automatic and manual RGC counting methods